SABA Publishing

Journal of Mathematical Analysis and Modeling
jmam.sabapub.com
ISSN 2709-5924

J Math Anal & Model
(2024)5(2) : 64-80
doi:10.48185/jmam.v5i2.1111

A-stable optimal hybrid linear multistep formulas in Runge-Kutta form and their application to dynamical systems

OLABODE B. T. [a], MOMOH A. L. [b,*],

[a,b] Federal University of Technology, Akure, Nigeria

• *Received: 10 April 2024* • *Accepted: 07 June 2024* • *Published Online: 29 June 2024*

Abstract

A-stable optimal hybrid Linear Multistep Formulas (LMFs) are developed and reformulated as Runge-Kutta-type schemes because of their excellent properties in handling the numerical solution of stiff differential equations. The LMFs are obtained using collocation and interpolation techniques and are reformulated as Runge-Kutta-type schemes via Butcher tableau. The resulting methods, when analyzed, have algebraic order six, and the A-stability characteristics of the proposed schemes are established. Newton's algorithm was adopted to handle the implicit nature of the suggested methods. The reformulated schemes are applied to Lorenz, Chau, Rossler, and Chen systems and four other standard stiff problems in the cited literature. A comparative study between the new method and the Dormand Prince scheme, popularly called ode45 in Matrix Laboratory (MatLab), is presented. The experiments demonstrate the latest methods' performance, indicating their potential for high accuracy and competitiveness with other established codes.

Keywords: Convergence analysis, Order, Local Truncation error, Wavelet Newton approach, Block method.
2010 MSC: 2010 (MSC) 65L04, 65L05, 65L06, 65L20.

1. Introduction

Two-parameter hybrid formulas of multistep nature are derived and reformulated as RK-type methods for solving chaotic and stiff differential systems. These usually occur in the application as a m-dimensional differential equations system.

$$\frac{dY}{dt} = F(Y,t), \tag{1.1}$$

where

$$F(Y,t) = \begin{pmatrix} f_1(y_1, y_2, \cdots, y_m) \\ f_2(y_1, y_2, \cdots, y_m) \\ \vdots \\ f_n(y_1, y_2, \cdots, y_m) \end{pmatrix}$$

*Corresponding author: almomoh@futa.edu.ng

Note that function f_i for all $i = 1, 2, \cdots, m$ are real-valued functions of variables $y_1, y_2, \cdots, y_n$ and t which are responsible for the local dynamics. The solution of (1.1) is a function of the type $Y(t) = (y_1(t), y_2(t), \cdots, y_n(t))$, so that

$$Y'(t) = F(Y(t), t), \tag{1.2}$$

where $Y'(t) = (y_1'(t), y_2'(t), \cdots, y_n'(t))$.

Because equation (1.1) is so complex, approximate solutions are frequently sought using two well-known numerical methods, namely the Runge-Kutta (see [1, 2, 3]) and Linear Multistep methods (LMMs). Furthermore, the likely extension of Euler's method by allowing the approximate solution at a mesh point to be determined by solution and derivative values at multiple previous step values resulted in Linear Multistep Methods (LMMs) (see [4], [5], [6], [7], [8], [9]).
The idea of predictor-corrector arose due to the LMM's implicit nature. Milne first introduced the Block method in 1926 as a way of providing starting values for Runge-Kutta (RK) methods(see [6]), and it was later adopted as a major implementation strategy for implicit LMM in subsequent literature. [10], [11], [12], [13], [14], [15], [16] and [17].

A one-step two-parameter hybrid continuous scheme is formulated as a unique block of four formulas. The methods are parameterized by replacing the grid index i in x_{n+i} with u and v, respectively. This generalization allows for different choices of u and v. Three choices of parameters u and v are considered, which resulted in three different internal stages of the suggested RK methods. One is the calculation of the two arbitrary points u and v through which the local truncation error of the proposed method is optimized. Following a similar strategy used by [16], the arbitrary points are obtained to minimize the local truncation errors of the formulas at the mesh points $x_{n+\frac{1}{2}}$ and x_{n+1}. The rest of this paper is structured as follows; Section 2 is devoted entirely to the derivation and specification of the proposed numerical integrator that gives the approximation $y(x)$ to the equation of type (1.1). Next, the method is examined in section 3 using the basic properties of LMMs, and numerical examples are provided in section 4. Finally, the paper is concluded in section 5, with some further relevant data presented in the appendix.

2. The Methodology and Suggested Methods

The true solution $y(x)$ is considered to be approximated by a polynomial $p(x)$. The coefficients of this polynomial are given in terms of approximate values of y and f at the different grid and off-grid points, including unevenly spaced function values. h is the constant step size considered, that is, $h = x_{j+1} - x_j$. The notations y_j and $f_j = f(x_j, y_j)$ are approximations, respectively, for the true values $y(x_j)$ and $y'(x_j) = f(x_j, y(x_j))$. The grid points considered is given by x_n, $x_{n+j} = x_n + jh$. Consider the true solution $y(x)$ is approximated by a polynomial $p(x)$ thus

$$y(x) \approx p(x) = \sum_{j=0}^{\infty} \tau_j x^j \tag{2.1}$$

where $\tau_j \in \mathcal{R}$ are real unknown coefficients to be determined. Therefore, the partial sum of (2.1) is obtained as

$$y(x) \approx p(x) = \sum_{j=0}^{k} \tau_j x^j \tag{2.2}$$

and its first derivative

$$y'(x) \approx p'(x) = \sum_{j=0}^{k} j\tau_j x^{j-1}. \tag{2.3}$$

where, $k = (I + C) - 1$, I and C denote number of interpolation and collocation points respectively. The approximating polynomial in (2.2) is imposed to be applied to the point x_n and that the first derivative in (2.3) applied to the points x_{n+j}, $j = 0,\ u,\ \frac{1}{2},\ v,\ 1$ coincide with the approximate solutions. This leads to a system of equations with six (6) unknown coefficients $(\tau_j,\ j = 0, 1, \cdots, 5)$ given by

$$\left.\begin{aligned} y_n &= p(x_n) \\ &\vdots \\ f_{n+j} &= p'(x_{n+j})\ ,\ j = 0,\ u,\ \tfrac{1}{2},\ \ v,\ 1 \end{aligned}\right\} \tag{2.4}$$

The above system of equations can be rewritten in matrix form as

$$\begin{pmatrix} 1 & x_n & x_n^2 & x_n^3 & x_n^4 & x_n^5 \\ 0 & 1 & 2x_n & 3x_n^2 & 4x_n^3 & 5x_n^4 \\ 0 & 1 & 2x_{n+u} & 3x_{n+u}^2 & 4x_{n+u}^3 & 5x_{n+u}^4 \\ 0 & 1 & 2x_{n+\frac{1}{2}} & 3x_{n+\frac{1}{2}}^2 & 4x_{n+\frac{1}{2}}^3 & 5x_{n+\frac{1}{2}}^4 \\ 0 & 1 & 2x_{n+v} & 3x_{n+v}^2 & 4x_{n+v}^3 & 5x_{n+v}^4 \\ 0 & 1 & 2x_{n+1} & 3x_{n+1}^2 & 4x_{n+1}^3 & 5x_{n+1}^4 \end{pmatrix} \begin{pmatrix} \tau_0 \\ \tau_1 \\ \tau_2 \\ \tau_3 \\ \tau_4 \\ \tau_5 \end{pmatrix} = \begin{pmatrix} y_n \\ f_n \\ f_{n+u} \\ f_{n+\frac{1}{2}} \\ f_{n+v} \\ f_{n+1} \end{pmatrix}. \tag{2.5}$$

Solving (2.5) for the unknown parameters (a_j)'s yields the required coefficients of the polynomial $p(x)$ in term of $y_n,\ f_n,\ f_{n+u},\ f_{n+\frac{1}{2}},\ f_{n+v},\ f_{n+1}$. After using the substitution $x = x_n + th$, the polynomial that approximates the solution may be written as

$$p(t) \ = \ \alpha_0 y_n + h(\beta_0 f_n + \beta_u f_{n+u} + \beta_{\frac{1}{2}} f_{n+\frac{1}{2}} + \beta_v f_{n+v} + \beta_1 f_{n+1}). \tag{2.6}$$

The coefficients $\alpha_0,\ \beta_0,\ \beta_u,\ \beta_{\frac{1}{2}},\ \beta_v,\ \beta_1$ define the method. Evaluating $p(t)$ at $t = u,\ \frac{1}{2},\ v,\ 1$ yield two parameter family of hybrid methods given by

$$\begin{aligned} y_{n+u} \ = \ & y_n + -\frac{1}{60}\Bigg(\frac{uh\left(6u^3 - 10u^2v - 15u^2 + 30uv + 10u - 30v\right) f_n}{v} \\ & + \ \frac{uh\left(24u^3 - 30u^2v - 45u^2 + 60uv + 20u - 30v\right) f_{n+u}}{(u-1)(-1+2u)(u-v)} \\ & + \ \frac{8\left(3u^2 - 5uv - 5u + 10v\right) hu^3 f_{n+\frac{1}{2}}}{(-1+2u)(2v-1)} + \frac{hu^3\left(6u^2 - 15u + 10\right) f_{n+v}}{(v-1)(2uv - 2v^2 - u + v)v} \\ & - \ \frac{hu^3\left(6u^2 - 10uv - 5u + 10v\right) f_{n+1}}{(v-1)(u-1)} \Bigg) \end{aligned} \tag{2.7}$$

$$
\begin{aligned}
y_{n+\frac{1}{2}} &= y_n + -\frac{1}{960}\Bigg(\frac{h\,(200\,uv-30\,u-30\,v+7)\,f_n}{uv} - \frac{h\,(30\,v-7)\,f_{n+u}}{(u-1)\,u\,(-1+2\,u)\,(u-v)} \\
&+ \frac{16\,(80\,uv-25\,u-25\,v+9)\,hf_{n+\frac{1}{2}}}{(-1+2\,u)\,(2\,v-1)} + \frac{h\,(30\,u-7)\,f_{n+v}}{(v-1)\,(2\,uv-2\,v^2-u+v)\,v} \\
&- \frac{h\,(40\,uv-10\,u-10\,v+3)\,f_{n+1}}{(v-1)\,(u-1)}\Bigg) \qquad (2.8)\\
y_{n+v} &= y_n + \frac{1}{60}\Bigg(\frac{vh\left(10\,uv^2-6\,v^3-30\,uv+15\,v^2+30\,u-10\,v\right)f_n}{u} \\
&- \frac{v^3h\left(6\,v^2-15\,v+10\right)f_{n+u}}{(u-1)\,u\,(-1+2\,u)\,(u-v)} - 16\,\frac{\left(5\,uv-3\,v^2-10\,u+5\,v\right)hv^3f_{n+\frac{1}{2}}}{(-1+2\,u)\,(2\,v-1)} \\
&+ \frac{vh\left(30\,uv^2-24\,v^3-60\,uv+45\,v^2+30\,u-20\,v\right)f_{n+v}}{(v-1)\,(2\,uv-2\,v^2-u+v)} \\
&- \frac{v^3h\left(10\,uv-6\,v^2-10\,u+5\,v\right)f_{n+1}}{(v-1)\,(u-1)}\Bigg) \qquad (2.9)\\
y_{n+1} &= y_n + \frac{1}{60}\Bigg(\frac{h\,(10\,uv-1)\,f_n}{uv} - \frac{hf_{n+u}}{(u-1)\,u\,(-1+2\,u)\,(u-v)} \\
&- \frac{16\,(10\,uv-5\,u-5\,v+3)\,hf_{n+\frac{1}{2}}}{(-1+2\,u)\,(2\,v-1)} + \frac{hf_{n+v}}{(v-1)\,(2\,uv-2\,v^2-u+v)\,v} \\
&+ \frac{h\,(10\,uv-10\,u-10\,v+9)\,f_{n+1}}{(v-1)\,(u-1)}\Bigg). \qquad (2.10)
\end{aligned}
$$

The choice of hybrid points depends on the number of partitions within the integration interval. The block linear multistep formulas ((2.7)-(2.10) are characterized by Butcher tableau as follows,

0	0	0	0	0	0
u	$\beta_{01}(u,v)$	$\beta_{02}(u,v)$	$\beta_{03}(u,v)$	$\beta_{04}(u,v)$	$\beta_{05}(u,v)$
$\frac{1}{2}$	$\beta_{11}(u,v)$	$\beta_{12}(u,v)$	$\beta_{13}(u,v)$	$\beta_{14}(u,v)$	$\beta_{15}(u,v)$
v	$\beta_{21}(u,v)$	$\beta_{22}(u,v)$	$\beta_{23}(u,v)$	$\beta_{24}(u,v)$	$\beta_{25}(u,v)$
1	$\beta_{31}(u,v)$	$\beta_{32}(u,v)$	$\beta_{33}(u,v)$	$\beta_{34}(u,v)$	$\beta_{35}(u,v)$
	$\beta_{31}(u,v)$	$\beta_{32}(u,v)$	$\beta_{33}(u,v)$	$\beta_{34}(u,v)$	$\beta_{35}(u,v)$

2.1. Methods with specified u and v values

When $u = \frac{1}{4}$ and $v = \frac{3}{4}$, we obtained an RK- scheme termed Symmetric Runge-Kutta SRK with the following tableau
Another choice of parameters u and v are zeros of Chebyshev polynomial of a first kind within the interval $[0,\ 1]$ given as $u = \dfrac{2-\sqrt{3}}{4}$, $v = \dfrac{2+\sqrt{3}}{4}$. This yields the RK-scheme termed Gauss Chebyshev Runge-Kutta with the following tableau

2.2. Optimal-hybrid block method

The two-parameters u and v can be uniquely determined by optimizing the local truncation error of the two-parameters block hybrid formulas for $y_{n+\frac{1}{2}}$ and y_{n+1}. The Taylor

0	0	0	0	0	0
$\frac{1}{4}$	$\frac{251}{2880}$	$\frac{323}{1440}$	$-\frac{11}{120}$	$\frac{53}{1440}$	$-\frac{19}{2880}$
$\frac{2}{4}$	$\frac{29}{360}$	$\frac{31}{90}$	$\frac{1}{15}$	$\frac{1}{90}$	$-\frac{1}{360}$
$\frac{3}{4}$	$\frac{27}{320}$	$\frac{51}{160}$	$\frac{9}{40}$	$\frac{21}{160}$	$-\frac{3}{320}$
1	$\frac{7}{90}$	$\frac{16}{45}$	$\frac{2}{15}$	$\frac{16}{45}$	$\frac{7}{90}$
1	$\frac{7}{90}$	$\frac{16}{45}$	$\frac{2}{15}$	$\frac{16}{45}$	$\frac{7}{90}$

Table 1: Butcher array representation of SRK method

0	0	0	0	0	0
u	$\frac{(-11+12\sqrt{3})}{320}$	$\frac{(256-117\sqrt{3})}{1440}$	$-\frac{(-88+51\sqrt{3})}{360}$	$\frac{(256-147\sqrt{3})}{1440}$	$\frac{(-21+12\sqrt{3})}{320}$
$\frac{1}{2}$	$-\frac{7}{40}$	$\frac{(16+15\sqrt{3})}{90}$	$\frac{11}{45}$	$-\frac{(-16+15\sqrt{3})}{90}$	$\frac{3}{40}$
v	$\frac{-(11+12\sqrt{3})}{320}$	$\frac{(256+147\sqrt{3})}{1440}$	$\frac{(88+51\sqrt{3})}{360}$	$-\frac{(256+117\sqrt{3})}{1440}$	$-\frac{(21+12\sqrt{3})}{320}$
1	$-\frac{1}{10}$	$\frac{16}{45}$	$\frac{22}{45}$	$\frac{16}{45}$	$-\frac{1}{10}$.
1	$-\frac{1}{10}$	$\frac{16}{45}$	$\frac{22}{45}$	$\frac{16}{45}$	$-\frac{1}{10}$.

Table 2: Butcher array representation of GCRK collocation method

series expansion of

$$\begin{aligned}\mathscr{L}(y(x_{n+\frac{1}{2}});h) &= y(x_n+\frac{h}{2})-\Bigg[y(x_n)+\frac{1}{960}\Bigg(\frac{h\,(200\,uv-30\,u-30\,v+7)\,y'(x_n)}{uv}\\ &- \frac{h\,(30\,v-7)\,y(x_n+uh)}{(u-1)\,u\,(-1+2\,u)\,(u-v)}\\ &+ \frac{16\,(80\,uv-25\,u-25\,v+9)\,hy'(x_n+\frac{h}{2})}{(-1+2\,u)\,(2\,v-1)}\\ &+ \frac{h\,(30\,u-7)\,y'(x_n+vh)}{(v-1)\,(2\,uv-2\,v^2-u+v)\,v}\\ &- \frac{h\,(40\,uv-10\,u-10\,v+3)\,y'(x_n+h)}{(v-1)\,(u-1)}\Bigg)\Bigg] \qquad (2.11)\end{aligned}$$

and

$$\begin{aligned}\mathscr{L}(y(x_{n+1});h) &= y(x_n+h)-\Bigg[y(x_n)+\frac{1}{60}\Bigg(\frac{h\,(10\,uv-1)\,y'(x_n)}{uv}\\ &- \frac{hy'(x_n+uh)}{(u-1)\,u\,(-1+2\,u)\,(u-v)}\\ &- \frac{16\,(10\,uv-5\,u-5\,v+3)\,hy'(x_n+\frac{h}{2})}{(-1+2\,u)\,(2\,v-1)}\\ &+ \frac{hy'(x_n+vh)}{(v-1)\,(2\,uv-2\,v^2-u+v)\,v}\\ &+ \frac{h\,(10\,uv-10\,u-10\,v+9)\,y'(x_n+h)}{(v-1)\,(u-1)}\Bigg).\Bigg] \qquad (2.12)\end{aligned}$$

about x_n yields after some simplification the following truncation errors:

$$\mathscr{L}(y(x_{n+\frac{1}{2}});h) = \frac{1}{230400}\,(30\,uv-7\,u-7\,v+2)\,y^{(6)}\,(x_n)\,h^6+O\left(h^7\right) \qquad (2.13)$$

$$\mathscr{L}(y(x_{n+1});h) = \frac{1}{14400}\,(u+v-1)\,y^{(6)}\,(x_n)\,h^6+O\left(h^7\right) \qquad (2.14)$$

Equating to zero the principal terms of the local truncation errors given in (2.13) and (2.14) respectively and solving simultaneously yields the optimal values of u and v as stated below $u=\frac{3-\sqrt{3}}{6}$, $v=\frac{3+\sqrt{3}}{6}$. It is observed that the values are the zeros of the first Legendre polynomial in the interval [0 1]. Hence, we obtained the RK scheme termed Gauss Legendre Runge-Kutta with the following tableau

	0	0	0	0	0
u	$\frac{(81+2\sqrt{3})}{1080}$	$\frac{(18+\sqrt{3})}{120}$	$-\frac{(-18+14\sqrt{3})}{135}$	$\frac{(-6+3\sqrt{3})}{40}$	$\frac{(-9+2\sqrt{3})}{1080}$
$\frac{1}{2}$	$\frac{31}{480}$	$\frac{(24+15\sqrt{3})}{160}$	$\frac{2}{15}$	$-\frac{h\,(-24+15\sqrt{3})}{160}$	$\frac{1}{480}$
v	$\frac{(81-2\sqrt{3})}{1080}$	$\frac{3\,h\,(2+\sqrt{3})}{40}$	$\frac{2\,h\,(9+7\sqrt{3})}{135}$	$-\frac{h\,(-18+\sqrt{3})}{120}$	$-\frac{h\,(9+2\sqrt{3})}{1080}$
1	$\frac{1}{15}$	$\frac{3}{10}$	$\frac{4}{15}$	$\frac{3}{10}$	$\frac{1}{15}$
1	$\frac{1}{15}$	$\frac{3}{10}$	$\frac{4}{15}$	$\frac{3}{10}$	$\frac{1}{15}$.

Table 3: Butcher array representation of GLRK method

3. Characteristics of the method

In this section, the suggested method is analyzed based on the following properties of the linear multistep method: local truncation error and order, zero stability, consistency,

convergence, and region of absolute stability.

3.1. Local truncation error and order

Assuming that $B(x)$ is a sufficiently differentiable function, the linear difference operators associated with (2.6) can be written in the form

$$\mathfrak{L}[B(x);h] \equiv \sum_{j=u,\frac{1}{2},v,1} \left[\alpha_j^1 B(x+jh) - \alpha_j^0 B(x+(j-h)) - \beta_j^0 B'(x+(j-h)) - \beta_j^1 B'(x+jh)\right], \tag{3.1}$$

where α_j^0, α_j^1, $\beta_j^0$and β_j^1 are respectively, for each index j in the summation, the vector columns of the matrices $\bar{A}_1$, $\bar{A}_0$, $\bar{B}_1$ and $\bar{B}_0$. Taking $B(x)$ as the true solution of the problem in (1.1), after expanding (3.1) in Taylor series about x yields the truncation errors of the form

$$\mathfrak{L}[B(x);h] = c_0^i B(x) + c_1^i h B'(x) + c_2^i h^2 B''(x) + \cdots + c_j^i h^j B^{(j)}(x) + O\left(h^{(j+1)}\right) \tag{3.2}$$

where c_j^i are column vectors.It is important to note that the first $p+1$ constants will be equal to zero, which means that

$$c_0^i = c_1^i = c_2^i = \cdots = c_p^i = 0, \text{ and } c_{p+1}^i \neq 0,$$

this implies that

$$\mathfrak{L}[B(x);h] = c_{p+1}^i h^{p+1} y^{p+1}(x) + O\left(h^{p+2}\right)$$

where p and c_{p+1}^i are respectively known as the order and local principal error constant of the corresponding formula. Applying (3.1) to the two-parameter continuous hybrid scheme (2.6) by expanding each term of the scheme in the Taylor series about x_n, which yields after some simplifications

$$\begin{aligned}\mathfrak{L}[B(x);h] = \frac{1}{14400}\,&(\,20t^4 - 24t^3u - 24t^3v + 30t^2uv - 36t^3 + 45t^2u + 45t^2v \\ &-60tuv + 15t^2 - 20tu - 20tv + 30uv)\,t^2 y^{(6)}(x_n)h^6 + O\left(h^7\right). \end{aligned}\tag{3.3}$$

Setting the parameter t in equation (3.3) to $t = u, \frac{1}{2}, v$ and 1 respectively, yields a system of equations that can be written as a column vector

$$\mathfrak{L}[B(x);h] = \begin{bmatrix} \frac{1}{14400}\left(-4u^4 + 6u^3v + 9u^3 - 15u^2v - 5u^2 + 10uv\right)u^2 y^{(6)}(x_n)h^6 + O\left(h^7\right) \\ \frac{1}{57600}\left(\frac{15}{2}uv - \frac{7}{4}u - \frac{7}{4}v + \frac{1}{2}\right)y^{(6)}(x_n)h^6 + O\left(h^7\right) \\ \frac{1}{14400}\left(6uv^3 - 4v^4 - 15uv^2 + 9v^3 + 10uv - 5v^2\right)v^2 y^{(6)}(x_n)h^6 + O\left(h^7\right) \\ \frac{1}{14400}\left(u + v - 1\right)y^{(6)}(x_n)h^6 + O\left(h^7\right) \end{bmatrix}. \tag{3.4}$$

By specifying the numerical values of u and v for each of the equations in (3.4), and upon further simplification yields the local truncation errors whose absolute value error constant are presented in figure 1. It is clear from figure 1 that GLRK has a lower absolute error constant than SRK and GCRK.

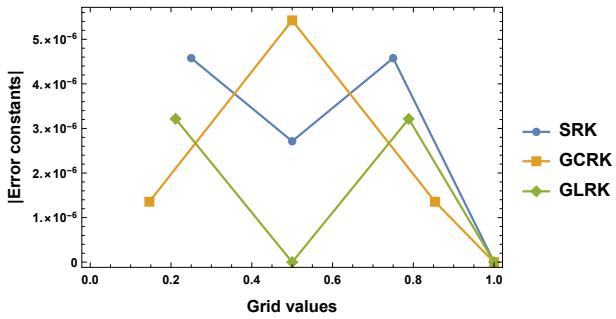

Figure 1: Absolute value of error constants versus grid values of the SRK, GCRK and GLRK

3.2. *Zero stability*

This kind of stability studies the behaviour of the block method when $h \to 0$. When this condition is applied to the two-parameter family of hybrid method ((2.7)-(2.10)), it reduces to formulas that can be written in matrix equation as

$$\bar{A}_1\, Y_m = \bar{A}_0\, Y_{m-1} \tag{3.5}$$

The two-parameter family of hybrid formulas ((2.7)-(2.10)) is said to zero-stable when the roots $\check{}_j$ of the characteristic polynomial $\mathbf{Q}_c$ given by $\mathbf{Q}_c = |\bar{A}_1\check{}_j - \bar{A}_0|$ satisfy $|\check{}_j| \leqslant 1$, and those roots with $|\check{}_j| = 1$, the multiplicity must not exceed one(1) Lambert (1973). $\mathbf{Q}_c = |\bar{A}_1\check{}_j - \bar{A}_0| = \lambda_j^3(\lambda_j - 1)$ solving for λ_j for $\mathbf{Q}_c = 0$, gives $\lambda_j = 0,\ 0,\ 0,\ 1$. Since $\lambda_j = 0,\ 0,\ 0,\ 1$, it is clear that the two parameter family of hybrid method ((2.7)-(2.10)) is zero stable.

3.2.1. *Analysis of the region of absolute stability of the methods*

Another characteristic of numerical methods other than zero-stability is linear stability which show the behavior of numerical methods when the step-size $h > 0$. [18] gives the linear test equation

$$y'(x) = \gamma y(x), \quad Re(\gamma) < 0 \tag{3.6}$$

as a way of obtaining the linear stability of numerical method for solving IVPs (1.1). Applying the linear test equation (3.6) to the two-parameter hybrid formulas ((2.7)-(2.10)) yields a system that can be represented in a matrix equation

$$\mathbf{Y} = M(\psi)\bar{\mathbf{Y}}, \quad \psi = \lambda h \tag{3.7}$$

where the amplification matrix $M(\psi)$ is given by

$$M(\psi) = \left(\bar{A}_1 - \psi\bar{B}_1\right)^{-1}\left(\bar{A}_0 + \psi\bar{B}_0\right) \tag{3.8}$$

where $\bar{A}_0,\ \bar{A}_1,\ \bar{B}_0$ and $\bar{B}_1$ are as defined before. Matrix (3.8) has eigenvalues

$$\{\varpi_1,\ \varpi_2,\ \varpi_3,\ \cdots,\ \varpi_k,\} = \{0,\ 0,\ 0,\ \cdots,\ \varpi_k,\}, \tag{3.9}$$

where the dominant eigenvalue ϖ_k is the stability function. Let $\varpi_k = R(\psi) : \mathbb{C} \to \mathbb{C}$. Applying the proposed methods to (3.7) and express in term of (3.8) yields after some

calculation the following stability function of the respective methods:

$$\mathbb{R}(\psi)_{SRK} = \frac{1+\frac{1}{2}\psi+\frac{7}{64}\psi^2+\frac{5}{384}\psi^3+\frac{1}{1280}\psi^4}{1-\frac{1}{2}\psi+\frac{7}{64}\psi^2-\frac{5}{384}\psi^3+\frac{1}{1280}\psi^4},$$

$$\mathbb{R}(\psi)_{GCRK} = \frac{1+\frac{1}{2}\psi+\frac{33}{320}\psi^2+\frac{19}{1920}\psi^3+\frac{1}{3840}\psi^4}{1-\frac{1}{2}\psi+\frac{33}{320}\psi^2-\frac{19}{1920}\psi^3+\frac{1}{3840}\psi^4},$$

$$\mathbb{R}(\psi)_{GLRK} = \frac{1+\frac{1}{2}\psi+\frac{13}{120}\psi^2+\frac{1}{80}\psi^3+\frac{1}{1440}\psi^4}{1-\frac{1}{2}\psi+\frac{13}{120}\psi^2-\frac{1}{80}\psi^3+\frac{1}{1440}\psi^4}.$$

The region of absolute stability $\mathbb{S}$ is defined as $\mathbb{S} = \{\psi \in \mathbb{C} : |Re(\psi)| \leqslant 1\}$. The stability region contains the entire left half complex plane and therefore, the method is A-stable [19, 20, 21, 16]. The SRK, GCRK and GLRK stability regions are shown in figures 2, 3 and 4. Method SRK, GCRK and GLRK have an unbounded stability region, including the complex plane's left-hand half-plane. From figures 2, 3 and 4, it can be seen that all the poles of the stability function are on the right-hand side, and all its zeros fall on the left-hand side of the complex plan. In figures 2, 3 and 4, $\Diamond$ represents Zeroes of polynomial $\mathbb{D}(\psi)$ while $\square$ represents Poles of polynomial $\mathbb{N}(\psi)$.

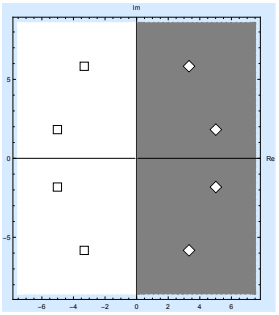

Figure 2: Region of absolute stability of SRK

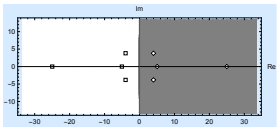

Figure 3: Region of absolute stability of GCRK

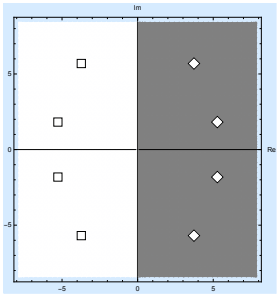

Figure 4: Region of absolute stability of GLRK

3.2.2. Further criteria for A-Stability

Let proceed by expressing the stability function as $\mathbb{R}(\psi) = \frac{\mathbb{N}(\psi)}{\mathbb{D}(\psi)}$. The following definition and theorem are important.

Definition 3.1

The E-polynomial of a Runge-Kutta method is $\mathbb{E}(y) = \mathbb{D}(iy)\,\mathbb{D}(-iy) - \mathbb{N}(iy)\,\mathbb{N}(-iy)$.

Theorem 3.1. *([19]) A Runge–Kutta method with stability function* $\mathbb{R}(\psi) = \frac{\mathbb{N}(\psi)}{\mathbb{D}(\psi)}$ *is A-stable if and only if (a) all poles of* $\mathbb{R}(\psi)$ *(that is, all zeros of* $\mathbb{D}$*) are in the right half-plane and (b)* $\mathbb{E}(y) \geqslant 0$*, for all real* y*.*

The suggested methods SRK, GCRK and GLRK satisfy the conditions stated in theorem 3.1. This is established by proving that the polynomial

$$\mathbb{E}(y) = \mathbb{D}(iy)\,\mathbb{D}(-iy) - \mathbb{N}(iy)\,\mathbb{N}(-iy) = 0$$

for each of the suggested methods. Consider

$$\begin{aligned}(\mathbb{D}(iy)\,\mathbb{D}(-iy))_{GLRK} &= \left(1-\frac{1}{2}\,iy-\frac{13}{120}\,y^2+\frac{1}{80}\,iy^3+\frac{1}{1440}\,y^4\right)\\ &\times\left(1+\frac{1}{2}\,iy-\frac{13}{120}\,y^2-\frac{1}{80}\,iy^3+\frac{1}{1440}\,y^4\right),\\ &= 1+\frac{1}{30}\,y^2+\frac{1}{1600}\,y^4+\frac{1}{172800}\,y^6+\frac{1}{2073600}\,y^8\end{aligned} \tag{3.10}$$

and

$$\begin{aligned}(\mathbb{N}(iy)\,\mathbb{N}(-iy))_{GLRK} &= \left(1+\frac{1}{2}\,iy-\frac{13}{120}\,y^2-\frac{1}{80}\,iy^3+\frac{1}{1440}\,y^4\right)\\ &\times\left(1-\frac{1}{2}\,iy-\frac{13}{120}\,y^2+\frac{1}{80}\,iy^3+\frac{1}{1440}\,y^4\right),\\ &= 1+\frac{1}{30}\,y^2+\frac{1}{1600}\,y^4+\frac{1}{172800}\,y^6+\frac{1}{2073600}\,y^8,\end{aligned}$$

therefore,

$$\begin{aligned}(\mathbb{E}(y))_{GLRK} &= \left(1+\frac{1}{30}\,y^2+\frac{1}{1600}\,y^4+\frac{1}{172800}\,y^6+\frac{1}{2073600}\,y^8\right)\\ &-\left(1+\frac{1}{30}\,y^2+\frac{1}{1600}\,y^4+\frac{1}{172800}\,y^6+\frac{1}{2073600}\,y^8\right)=0.\end{aligned}$$

The following $\mathbb{E}(y)$ polynomial are obtained for SRK and GCRK.

$$\begin{aligned}(\mathbb{E}(y))_{SRK} &= \left(1+\frac{1}{32}\,y^2+\frac{31}{61440}\,y^4-\frac{1}{737280}\,y^6+\frac{1}{1638400}\,y^8\right)\\ &-\left(1+\frac{1}{32}\,y^2+\frac{31}{61440}\,y^4-\frac{1}{737280}\,y^6+\frac{1}{1638400}\,y^8\right)=0,\\ (\mathbb{E}(y))_{GCRK} &= \left(1+\frac{7}{160}\,y^2+\frac{129}{102400}\,y^4+\frac{163}{3686400}\,y^6+\frac{1}{14745600}\,y^8\right)\\ &-\left(1+\frac{7}{160}\,y^2+\frac{129}{102400}\,y^4+\frac{163}{3686400}\,y^6+\frac{1}{14745600}\,y^8\right)=0\end{aligned}$$

These results confirm that the proposed method SRK, GCRK and GLRK are A-stable.

4. Numerical Examples

Some numerical experiments with the following problems are presented to study the efficiency of the developed methods. Methods SRK, GCRK, and GLRK are applied to solve the following test problems:

4.1. Example 1

The Kap problem

$$\begin{cases} \dfrac{dx}{dt} &= -1002x + 1000y^2, \quad x(0) = 1, \\ \dfrac{dy}{dt} &= -x - y(1+y), \qquad y(0) = 1 \end{cases} \tag{4.1}$$

whose exact solution are $x(t) = e^{-2t}$ and $y(t) = e^{-t}$ which have appeared in [23], Khalsaraei *et al.* [24] and Adewale *et al.* [25].

Table 4: Comparison of absolute errors of example 4.1

x	y_i	Absolute Errors in			
		SRK, $p = 6$	GCRK, $p = 6$	GLRK, $p = 6$	[23], $p = 10$
5	y_1	7.61502×10^{-13}	6.31717×10^{-14}	6.23612×10^{-13}	5.82586×10^{-2}
	y_2	1.33227×10^{-15}	3.44169×10^{-15}	3.33067×10^{-16}	3.22596×10^{-2}
50	y_1	2.29053×10^{-14}	7.63278×10^{-17}	1.82909×10^{-14}	6.73588×10^{-3}
	y_2	3.71925×10^{-15}	6.38378×10^{-15}	2.08167×10^{-15}	2.61819×10^{-2}
150	y_1	8.40087×10^{-18}	1.15112×10^{-18}	6.56959×10^{-18}	2.46861×10^{-6}
	y_2	2.07733×10^{-16}	3.45644×10^{-16}	1.21864×10^{-16}	5.36088×10^{-4}
250	y_1	2.86204×10^{-21}	9.72764×10^{-22}	2.1395×10^{-21}	8.16361×10^{-10}
	y_2	4.24872×10^{-18}	1.25361×10^{-17}	1.56532×10^{-18}	9.75975×10^{-6}
500	y_1	5.34939×10^{-24}	3.24109×10^{-24}	5.34939×10^{-24}	1.61659×10^{-18}
	y_2	1.65436×10^{-23}	1.51002×10^{-21}	1.65436×10^{-23}	4.34317×10^{-10}

Table 5: Comparison of absolute errors of example 4.1

x	h	Absolute Errors in				
		y_i	SRK, $p = 6$	GCRK, $p = 6$	GLRK, $p = 6$	Adewale *et al.* [25], $p = 8$
10	0.1	y_1	1.69×10^{-18}	1.66×10^{-19}	1.23×10^{-18}	1.40×10^{-11}
		y_2	1.55×10^{-15}	2.79×10^{-15}	8.25×10^{-16}	4.79×10^{-08}
	0.05	y_1	1.24×10^{-20}	2.92×10^{-21}	9.43×10^{-21}	8.86×10^{-12}
		y_2	2.35×10^{-17}	4.14×10^{-17}	1.25×10^{-17}	3.10×10^{-08}
	0.001	y_1	6.07×10^{-22}	5.66×10^{-22}	5.84×10^{-22}	3.40×10^{-13}
		y_2	5.14×10^{-18}	4.68×10^{-18}	4.89×10^{-18}	1.28×10^{-09}
15	0.1	y_1	1.69×10^{-18}	1.66×10^{-19}	1.23×10^{-18}	6.34×10^{-16}
		y_2	1.55×10^{-15}	2.79×10^{-15}	8.25×10^{-16}	3.23×10^{-10}
	0.05	y_1	1.24×10^{-20}	2.92×10^{-21}	9.43×10^{-21}	4.02×10^{-16}
		y_2	2.35×10^{-17}	4.14×10^{-17}	1.25×10^{-17}	2.09×10^{-10}
	0.001	y_1	6.07×10^{-22}	5.66×10^{-22}	5.84×10^{-22}	1.54×10^{-17}
		y_2	5.14×10^{-18}	4.68×10^{-18}	4.89×10^{-18}	8.64×10^{-12}

4.2. Example 2

$$\begin{cases} \dfrac{dx}{dt} = \lambda x + y^2, \quad x(0) = \frac{-1}{\lambda+2}, \\ \dfrac{dy}{dt} = y, \qquad y(0) = 1, \end{cases} \tag{4.2}$$

with exact solution $x(t) = \dfrac{-e^{-2t}}{\lambda+2}$ and $y(t) = e^{-t}$ where $\lambda = -10000$.This problem has appeared in Akinfenwa *et al.* [11], [26] and Khalsaraei *et al.*

Table 6: Comparison of absolute errors of example 4.2

x	Ey_i	SDMM ($h = 0.0001$) in [26]	$p = 6$ SRK, $h = 0.1$	GCRK, $h = 0.1$	GLRK, $h = 0.1$
3	y_1	2.478147×10^{-11}	1.2933×10^{-15}	6.2965×10^{-16}	1.1826×10^{-15}
3	y_2	2.471093×10^{-06}	5.0793×10^{-13}	9.1405×10^{-13}	2.7089×10^{-13}
5	y_1	3.450271×10^{-14}	2.2825×10^{-15}	1.0812×10^{-15}	2.0816×10^{-15}
5	y_2	2.304573×10^{-08}	8.3178×10^{-13}	1.4968×10^{-12}	4.4342×10^{-13}
10	y_1	3.456372×10^{-18}	3.9981×10^{-15}	1.9318×10^{-15}	3.6449×10^{-15}
10	y_2	3.456372×10^{-10}	1.1349×10^{-12}	2.0426×10^{-12}	6.0518×10^{-13}

4.3. Example 3

$$\begin{cases} \dfrac{dx}{dt} = 998x + 1998y, \quad x(0) = 1, \\ \dfrac{dy}{dt} = -999x - 1999y, \quad y(0) = 1, \end{cases} \tag{4.3}$$

with exact solution:$y_1(x) = 4e^{-x} - 3e^{-1000x}$ and $y_2(x) = -2e^{-x} + 3e^{-1000x}$.This can be found in [26].

Table 7: Comparison of absolute errors of example 4.3.

x	y_i	$BBDF_8$ in [26], $p = 8$	SRK, $p = 6$	GCRK, $p = 6$	GLRK, $p = 6$
	y_1	4.18×10^{-13}	8.2591×10^{-15}	1.10401×10^{-14}	2.27791×10^{-15}
10	y_2	2.09×10^{-13}	1.13284×10^{-14}	5.52001×10^{-15}	6.25829×10^{-16}

4.4. Example 4

$$\begin{cases} \dfrac{dx}{dt} &= -21x + 19y - 20z,\ x(0) = 1, \\ \dfrac{dy}{dt} &= 19x - 21y + 20z,\ y(0) = 0, \\ \dfrac{dz}{dt} &= 40x - 40y - 40z,\ z(0) = -1, \end{cases} \tag{4.4}$$

with tho following exact solutions $x(t) = 0.5e^{-2t} + 0.5e^{-40t}\left(\cos(40t) + \sin(40t)\right)$, $y(t) = 0.5e^{-2t} - 0.5e^{-40t}\left(\cos(40t) + \sin(40t)\right)$, and $z(t) = -e^{-40t}\left(\cos(40t) + \sin(40t)\right)$. The problem has also appeared in Yakubu *et al.* [27].

Table 8: Comparison of absolute errors of example 4.4

x	y_i	Radau IIA in [27]	Method (3.3) in [28]	GLRK
5	y_1	$2.60451549216612\times10^{-10}$	$4.650613227852318\times10^{-12}$	7.64944×10^{-13}
	y_2	$2.60451687994490\times10^{-10}$	$4.650606288958414\times10^{-12}$	7.65062×10^{-13}
	y_3	$1.07396436188623\times10^{-09}$	$3.083699962047604\times10^{-12}$	5.05873×10^{-13}
50	y_1	$2.78099765438355\times10^{-12}$	$1.150857187326437\times10^{-12}$	1.91902×10^{-13}
	y_2	$2.78099765438355\times10^{-12}$	$1.150857187326437\times10^{-12}$	1.92624×10^{-13}
	y_3	$3.96613819020217\times10^{-10}$	$2.303427004121455\times10^{-12}$	3.78384×10^{-13}
250	y_1	$8.32667268468867\times10^{-17}$	$1.942890293094024\times10^{-16}$	2.22045×10^{-16}
	y_2	$1.38777878078145\times10^{-16}$	$1.665334536937735\times10^{-16}$	3.60822×10^{-16}
	y_3	$1{:}99011769660684\times10^{-16}$	$7.896102966055376\times10^{-18}$	1.39475×10^{-17}
500	y_1	$1.11022302462516\times10^{-16}$	$9.714451465470120\times10^{-17}$	5.55112×10^{-17}
	y_2	$1.11022302462516\times10^{-16}$	$9.714451465470120\times10^{-17}$	4.16334×10^{-17}
	y_3	$6.23470886821874\times10^{-18}$	$5.606066530391557\times10^{-18}$	5.01899×10^{-18}

4.5. Example 5: The Lorenz system

The first chaotic processes to be considered here is the Lorenz system

$$\begin{cases} \dfrac{dx}{dt} &= a(y - x), \\ \dfrac{dy}{dt} &= cx - xz - y, \\ \dfrac{dz}{dt} &= xy - bz \end{cases} \tag{4.5}$$

which is chaotic when $a = 10$, $b = \frac{8}{3}$, $c = 28$ (see [29], [30], [31, 32, 33]). Figures 9 is the solution of the Lorenz equations for $\rho = 10$, $\beta = \frac{8}{3}$, $\sigma = 28$, initial conditions $y_1 = 1$, $y_2 = 4$, $y_3 = 9$ using optimal method and ode45 with time step $h = 0.01$ for 10000 steps. Figures (5-8) are phase space of y_1, y_2, and y_3 corresponding to Figure 9.

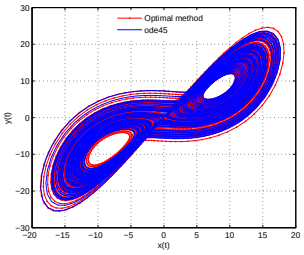

Figure 5: 2D phase portrait of Lorenz equation 4.5

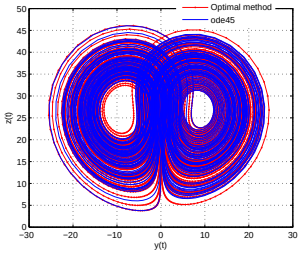

Figure 6: 2D phase portrait of Lorenz equation 4.5

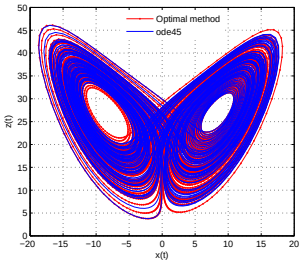

Figure 7: 2D phase portrait of Lorenz equation 4.5

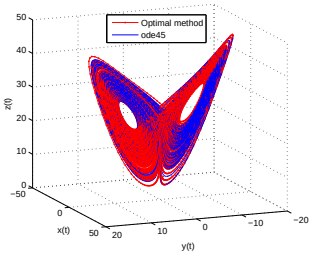

Figure 8: 3D phase portrait of Lorenz equation 4.5

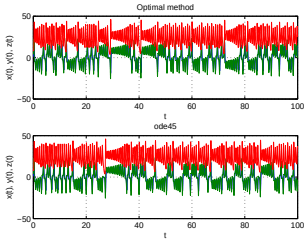

Figure 9: Solution curve for Lorenz equation 4.5

4.6. *Example 6: The Chua system*

The Chua system

$$\begin{cases} \dfrac{dx}{dt} &= A(y - g(x)), \\ \dfrac{dy}{dt} &= x - y + z, \\ \dfrac{dz}{dt} &= Bx - Cz \end{cases} \tag{4.6}$$

where

$$g(x) = xm_0 + \frac{1}{2}(m_0 - m_1)(|x+1| - |x-1|)$$

which is chaotic when $A = 10.1911$, $B = 10.3035$, $C = 0.1631$ is also considered see [34]

Figures 14 is the solution of the Chua equations for $A = 8.4562$, $B = 12.0732$, $C = 0.0052$, $m0 = 0.3532$, $m1 = -1.1468$, initial conditions $y_1 = 8.8200$, $y_2 = 0.5561$, $y_3 = -12.6008$ using optimal method and ode45 with time step $h = 0.001$ for 100000 steps. Figures (10-13) are phase space of y_1, y_2, and y_3 corresponding to Figure 9.

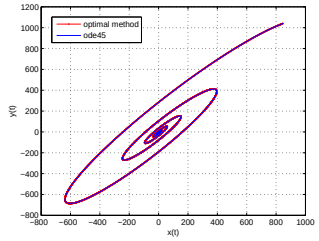

Figure 10: 2D phase portrait of Chua equation 4.6

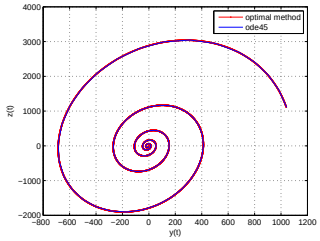

Figure 11: 2D phase portrait of Chua equation 4.6

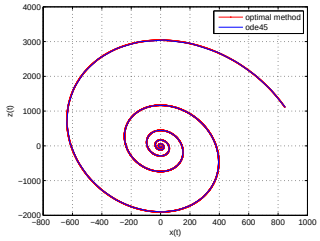

Figure 12: 2D phase portrait of Chua equation 4.6

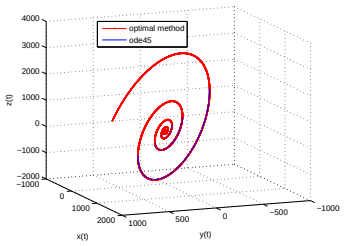

Figure 13: 3D phase portrait of Chua equation 4.6

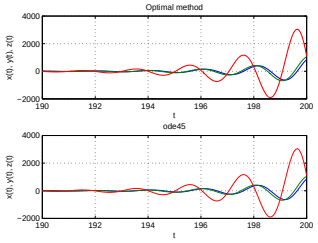

Figure 14: Solution curve for Chua equation

4.7. Example 7: The Rossler system

The third example is the Rossler system

$$\begin{cases} \dfrac{dx}{dt} &= -y - z, \\ \dfrac{dy}{dt} &= x + ay, \\ \dfrac{dz}{dt} &= xz - bz + c \end{cases} \tag{4.7}$$

which is chaotic when $a = 0.2,\ \ b = 5.7,\ \ c = 0.2$ see ([29], [30]). Figures 19 is the solution of the Rossler equations for $A = 0.2,\ B = 5.7,\ C = 0.2$, initial conditions $y_1 = 3.303857266661332e$, $y_2 = 5.752677509797773$, $y_3 = 2.138119394911370$ using optimal method and ode45 with time step $h = 0.001$ for 200000 steps. Figures (15-18) are phase space of y_1, y_2, and y_3 corresponding to Figure 9. Lorenz, Chua and Rossler systems are arbitrarily closely approximated by other locations with drastically differing future paths of trajectories, which is known as sensitivity to initial conditions. As a result, even a minor alteration or disruption of the current trajectory can result in drastically different future behaviour. The systems produce different effects depicted in the phase portrait shown in Figures 5 and 19. The Lorenz system produces butterfly effects.

5. Conclusion

This paper introduces implicit Runge-Kutta methods for solving chaotic and stiff initial-value problems. The resulting methods are A-stable and have an algebraic order of six.

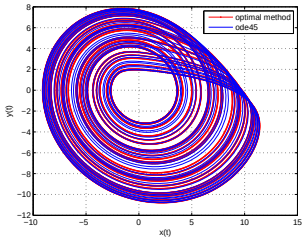

Figure 15: 2D phase portrait of Rossler equation 4.7

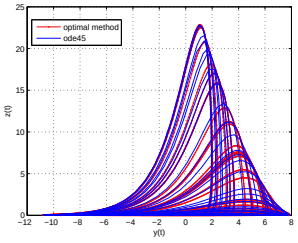

Figure 16: 2D phase portrait of Rossler equation 4.7

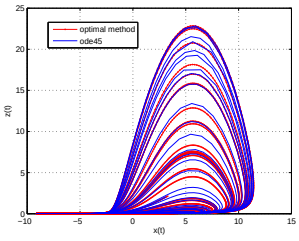

Figure 17: 2D phase portrait of Rossler equation 4.7

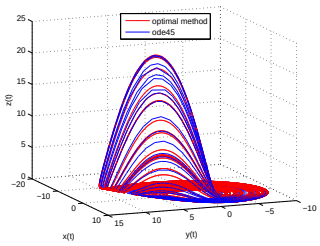

Figure 18: 3D phase portrait of Rossler equation 4.7

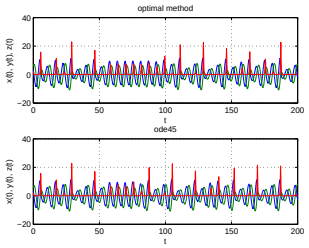

Figure 19: Solution curve for Rossler equation

Numerical examples suggest that these methods are promising and may be competitive with other commonly used codes for stiff differential equations. The results obtained compare well with those from standard software for simulating such problems.

Acknowledgement

The second author would like to thank Prof. G. D. Yakubu and the reviewers for their valuable contributions that have enhanced this paper.

References

[1] Ouncharoen R, Shah K, Ud Din R, Abdeljawad T, Ahmadian A, Salahshour S, and Thanin Sitthiwirattham. *Study of integer and fractional order covid-19 mathematical model*. Fractals, 31(4):2340046, 2023.

[2] Rabiei F, Abd Hamid F, Rashidi M M, Ali Z, Shah K, Hosseini K, and Khodadadi T. Numerical simulation of fuzzy volterra integro-differential equation using improved runge-kutta method. Journal of Applied and Computational Mechanics, 9(1):72–82, 2023.

[3] Duromola MK, Animasaun IL, Rufai MA, and Momoh AL. *Insight into 2-step continuous block method for solving mixture model and sir model.* International Journal of Computing Science and Mathematics, 14(4):347, 2021.

[4] Hairer E and Wanner G. *Solving Ordinary Differential Equations II*. Springer Berlin Heidelberg, 1996.

[5] Henrici P. *Discrete Variable Methods in Ordinary Differential Equations*. John Wiley and Sons Inc, New York, 1962.

[6] Milne WE.. *Numerical integration of ordinary differential equations*. Amer. Math., pages 455– 460, 1926.

[7] Curtiss CF and Hirschfelder JO. *Integration of stiff equations*. Proceedings of the National Academy of Sciences, 38(3):235–243, Mar 1952.

[8] Butcher JC. *Integration processes based on radau quadrature formulas*. Math. Comp., 18:233–244, 1964.

[9] Butcher JC. *The Numerical Methods for Ordinary Differential Equations*. Wiley and Son, Ltd, 2008.

[10] Fatunla SO. PREFACE. *In Numerical Methods for Initial Value Problems in Ordinary Differential Equations*, pages ix–xi. Elsevier, 1988.
[11] Akinfenwa AO, Akinnukawe B, and Mudasiru SB. *A family of continuous third derivative block methods for solving stiff systems of first order ordinary differential equations*. Journal of the Nigerian Mathematical Society, 34(2):160–168, Aug 2015.
[12] Agarwal P and Ibrahim IH. *A new type of hybrid multistep multiderivative formula for solving stiff IVPs*. Advances in Difference Equations, 2019(1), Jul 2019.
[13] Jator SN. *Implicit third derivative runge-kutta-nystrm method with trigonometric coefficients*. Numerical Algorithms, 70(1):133–150, nov 2014.
[14] Jator SO and Oladejo HB. *Block nystrm method for singular differential equations of the lane–emden type and problems with highly oscillatory solutions*. International Journal of Applied and Computational Mathematics, 3(S1):1385–1402, Sep 2017.
[15] Ramos H and Singh G. *A note on variable step-size formulation of a simpson's-type second derivative block method for solving stiff systems*. Applied Mathematics Letters, 64:101–107, Feb 2017.
[16] Ramos H. *Development of a new runge-kutta method and its economical implementation*. Computational and Mathematical Methods, 1(2): e1016, mar 2019.
[17] Olabode BT and Momoh AL. *Continuous hybrid multistep methods with legendre basis function for direct treatment of second order stiff odes*. America Journal of Computational and Applied Mathematics, 6:38–49, 2015.
[18] Dahlquist GG. *Stability questions for some numerical methods for ordinary differential equations*, 1963.
[19] Butcher JC. *The Numerical Analysis of Ordinary Differential Equations*. Wiley and Son, U. K., 2003.
[20] Butcher JC and Rattenbury N. *ARK methods for stiff problems*. Applied Numerical Mathematics, 53(2-4):165–181, May 2005.
[21] Butcher JC. *General linear methods*. Acta Numerica, 15:157, May 2006.
[22] Butcher JC and Cash JR. *Towards efficient runge–kutta methods for stiff systems*. SIAM Journal on Numerical Analysis, 27(3):753–761, Jun 1990.
[23] Yakubu GD and Markus S. *The efficiency of second derivative multistep methods for the numerical integration of stiff systems*. Journal of the Nigerian Mathematical Society, 35(1):107–127, Apr 2016.
[24] h Khalsaraei MM, Shokri A, and Molayi M. *The new class of multistep multiderivative hybrid methods for the numerical solution of chemical stiff systems of first order IVPs*. Journal of Mathematical Chemistry, 58(9):1987–2012, Jul 2020.
[25] James A, Adesanya O, Onsachi O, Sunday J, and Moses O. *Proficiency of second derivative schemes for the numerical solution of stiff systems*. American Journal of Computational Mathematics, 08(01):96–107, 2018.
[26] Akinfenwa AO. *Third derivative hybrid block integrator for solution of stiff systems of initial value problems*. Afrika Matematika, 28(3-4):629–641, Dec 2016.
[27] Yakubu GD, Aminu M and Aminu A. *The numerical integration of stiff systems using stable multistep multiderivative methods*. Journal of Modern Methods in Numerical Mathematics, 8(1-2):99, oct 2017.
[28] Yakubu GD. *Accurate multistep multi-derivative collocation methods applied to chaotic systems*. Journal of Modern Methods in Numerical Mathematics, 9(1-2):1–15, Mar 2018.
[29] Chen G and Ueta T. *Yet another chaotic attractor*. International Journal of Bifurcation and Chaos, 09(07):1465–1466, Jul 1999.
[30] Wang M. *Chaotic control of Lua system via three methods*. International Journal of Modern Nonlinear Theory and Application, 03(02):29–36, 2014.
[31] Lorenz EN. *Deterministic and stochastic aspects of atmospheric dynamics. In Irreversible Phenomena and Dynamical Systems Analysis in Geosciences*, pages 159–179. Springer Netherlands, 1987.
[32] Lorenz EN. *Deterministic nonperiodic flow. In The Theory of Chaotic Attractors*, pages 25–36. Springer New York, 2004.
[33] Lorenz EN. *Deterministic nonperiodic flow*. In Universality in Chaos, pages 367–378. CRC Press, Jul 2017.
[34] Leonov GA and Kuznetsov NV. *On differences and similarities in the analysis of lorenz, chen, and lu systems*. Applied Mathematics and Computation, 256:334–343, apr 2015.